A new phase transition in the T-P diagram of C_{60} fullerite

1994 J. Phys.: Condens. Matter 6 7491

(http://iopscience.iop.org/0953-8984/6/36/028)

J. Phys.: Condens. Matter 6 (1994) 7491–7498. Printed in the UK

A new phase transition in the T–P diagram of C_{60} fullerite

I O Bashkin†, V I Rashchupkin†, A F Gurov†, A P Moravsky‡,
O G Rybchenko†, N P Kobelev†, Ya M Soifer† and E G Ponyatovsky†

† Institute of Solid State Physics, Russian Academy of Sciences, 142432 Chernogolovka, Moscow District, Russia

‡ Institute of Chemical Physics, Russian Academy of Sciences, 142432 Chernogolovka, Moscow District, Russia

Received 6 June 1994

Abstract. The earlier high-pressure study of C_{60} concentrated on the orientational transition and room-temperature transformations observed in diamond anvils. This work presents a part of the T–P phase diagram for solid C_{60} at pressures up to 20 kbar in the temperature range extended to 700 K. A new phase region is outlined herein. The new phase is retained to ambient conditions and preliminarily characterized. The new phase is more dense than the initial C_{60} by at least 8.5% and less compressible by ~1.5 times. Its crystal structure is very different from the well known face-centred cubic and simple cubic phases, and its recovery to a cubic phase is associated with an endothermal heat effect of ~23 J g^{-1}. The nature and the thermodynamic stability of the new phase are discussed in connection with polymerization of C_{60} molecules, which seems likely.

1. Introduction

The unique molecular state of carbon in fullerenes gave rise to the intense study of their crystals, fullerites. Solid C_{60} has a closely packed face-centred cubic (FCC) crystal lattice at standard conditions, but transforms to the simple cubic (SC) phase between 252 and 258 K [1–8]. These crystal lattices differ only by the orientational order of the C_{60} molecules in the SC phase. The orientational transition results in a volume discontinuity of less than 1% (a = 14.154 Å for the FCC phase and a = 14.111 Å for the SC near 255 K) [3–5] as well as a small latent heat, $\Delta H \simeq 9.5$ J g^{-1} [6, 7]. The transition temperature, T_c, grows under hydrostatic pressure with a slope $dT_c/dP \simeq 11$ K $kbar^{-1}$ in helium atmosphere [7–9], but $dT_c/dP \simeq 16$ K $kbar^{-1}$ in pentane–isopentane or nitrogen media [8, 9]. Samara *et al* argued that higher values of the slope represented the intrinsic property, and He reduced the slope because He readily permeated into interstices of the C_{60} lattice [8].

In the range of extreme pressures, x-ray diffraction, infrared (IR) and Raman spectra have been measured at room temperature using diamond anvils. It was found that the C_{60} molecules were stable on hydrostatic compression to at least 200 kbar [10]. However, the sp^3-hybridized C–C bonds between the adjacent C_{60} molecules (reversible polymerization) arose even below 100 kbar under quasi-hydrostatic pressures or during long maintenance of C_{60} under hydrostatic pressures [11, 12]. Evolution of the process led to irreversible transformations to diamond, graphite or amorphous C in the range 200–300 kbar [12–16].

A volume jump, $\Delta V/V_0 \simeq 4.7\%$ has been recently observed near P = 6.7 kbar in pure C_{60} when its volume was measured in dependence on pressure at T = 557 K [17]. This was indicative of a new phase transition. In this work we studied the T–P phase diagram of solid C_{60} up to 20 kbar in the temperature range up to 700 K using compressibility

0953-8984/94/367491+08$19.50

measurements. The new high-pressure phase was retained and primarily characterized at atmospheric pressure.

2. Experimental details

A toluene extract of fullerene-rich soot was chromatographed on neutral alumina in the absence of light and oxygen. The C_{60} solution was concentrated in a rotary evaporator. Fine-grained crystals were precipitated with pentane, washed in ether, then recrystallized from toluene: pentane. Solvent was evacuated at 540 K in a vacuum of 10^{-5} Torr during 50 h. Neither C_{70} nor other impurities were found by high-performance liquid chromatography within its accuracy (<0.01%). There were no traces of the C–H vibration bands in the IR spectrum, nor did differential thermal gravimetry show any solvent.

All volume measurements were carried out on the same C_{60} sample as in [17] using a high-pressure piston-cylinder piezometer [18]. A 0.198 g sample was compacted as a cylinder of 4.8 mm diameter, encased in an aluminium cover of 6 mm diameter and mounted in the pressure cell of the piezometer. Piston displacements, $\Delta l(P, T)$, were registered with a dial gauge graduated every 1 μm and with an X–Y recorder. The rate of scanning within transition intervals was 0.1 kbar min^{-1}. The temperature was maintained constant within ± 1 K over a transition interval and within ± 5 K over a run. Friction in the pressure cell was 1.5 to 2 kbar over 470 K and about 3.5 kbar at 290 K. Both isothermal compression/decompression cycles and isobaric heating and cooling runs were employed to study the T–P diagram.

X-ray diffraction patterns were taken at room temperature using a D500 Siemens diffractometer with Cu Kα irradiation.

Heat capacity was measured on a sample of 35 mg weight using a Perkin-Elmer DSC7 calorimeter at a heating rate of 10 K min^{-1}. The calorimeter enabled measurements between 110 and 420 K in He flow and in the flow of spectrally pure argon over 350 K. He absorption effect on all parameters of the orientational transition were clearly observed in preliminary experiments. The sample was therefore cold welded in an Al ampoule before low-temperature runs. The same sample was treated under pressure in order to transform it to the new phase. However, it was necessary to pierce the Al ampoule before high-temperature runs because the sample left some free space in the ampoule, and a small amount of ambient atmosphere was sufficient to blast the ampoule at elevated temperatures. The sample was repacked in another ampoule when the low-temperature run followed the high-temperature one.

3. Results

3.1. The T–P phase diagram of C_{60}

Figure 1 exemplifies experimental pressure–volume relations observed at elevated temperatures. Figure 2 represents the transition from the high-pressure phase (we shall call it 'a new phase', for brevity) to FCC C_{60} at atmospheric pressure. The experimental transition parameters are summarized in the T–P diagram shown in figure 3.

Curves $\Delta l(P)$ in figure 1 show the total compressibility of the sample and the pressure cell. This shape of curves was normal for isothermal compressibility cycles over 550 K. Each curve included two intervals where displacements were accurately fitted with the second-order polynomials. Normal compressibility behaviour of C_{60} is implicit in these intervals. A volume discontinuity is evident at intermediate pressures, which is indicative

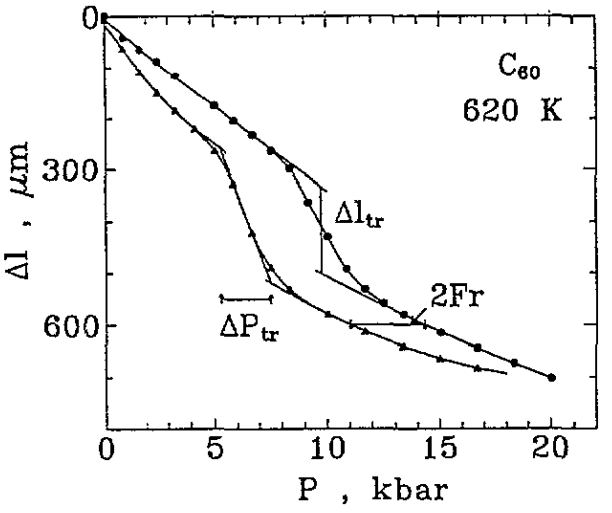

Figure 1. Piston displacements in dependence on pressure, $\Delta l(P)$, in the compressibility cycle at 620 K. Circles and triangles show the gauge readings in compression and decompression runs, respectively. The second-order polynomial fits in the intervals of normal compressibility are plotted. The transition pressures correspond to the inflection points. The transition intervals, ΔP_{tr}, are determined from intersection points of the inflectional tangents with fitting polynomials. All pressure values were corrected for friction, Fr, equal to a halfwidth of the hysteresis loop beyond the transition intervals. The length decrement due to the transition, Δl_{tr}, is a distance between fitting polynomials at the inflection.

of a phase transition in C_{60}. The relative volume jumps, $\Delta V/V_0$, were readily determined from these curves. Here $V_0 = 0.559$ cm^3 g^{-1} is the C_{60} specific volume calculated from the x-ray data at room temperature. The absolute values of the jumps ranged between 3.5 and 5.0% for isotherms over 550 K. These values were somewhat larger in decompression runs and decreased at higher temperatures, hence, at higher pressures. This is consistent with the phase diagram and with the lower compressibility of the new phase stated below.

The transition kinetics depended on temperature. The rate of the transition markedly decreased below 520 K. This led to reduction of the apparent volume jump. However, a further pressure-activated transition process was implicit on compression from the gauge drift at a fixed pressure far above the apparent transition interval, as shown in figure 3. The reverse transition at $T = 510$ K terminated near the normal pressure. Only the transition onset was observed on decompression at 470 K, and it was necessary to heat the sample to ~510 K to complete the process in a reasonable time.

Such behaviour indicated that the new phase could be retained from the region of its formation to ambient conditions. This was proved by slow (during 1.5 h) cooling of the sample from 700 to 290 K at a fixed pressure of 20 kbar followed by decompression to $P =$ 1 bar. Smooth curves $\Delta l(T)$ and $\Delta l(P)$ were observed in these runs, which ruled out phase transitions with a large volume jump, but a large volume jump did occur on subsequent heating of the sample at zero applied pressure (figure 2). Its average value from two heating runs is $\Delta V/V_0 = 8.5 \pm 0.3\%$.

It is clear from the experimental T–P diagram in figure 3 that the transition revealed is nearly irreversible in either direction below about 450 K. In contrast, good kinetics is characteristic of the transition over 570 K; its hysteresis linearly decreases to 700 K where it becomes negligible. Data from four cycles over 570 K were therefore used to estimate

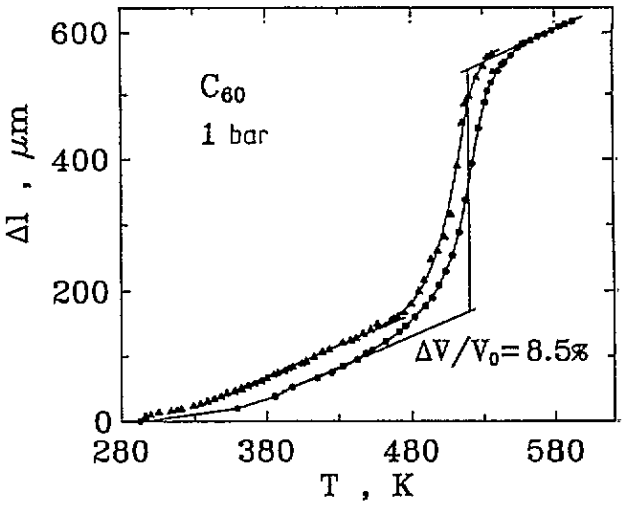

Figure 2. Piston displacements, $\Delta l(T)$, on heating the retained new phase of C_{60} at zero applied pressure. A small residual pressure is assumed due to friction. The heating run at a fixed supply voltage is shown with circles, and triangles are for the run at a hand-operated heating rate of about 0.7 K min^{-1}. The difference between the curves is due to different heating rates and thermal inertia of the pressure cell. Transition temperatures, transition intervals and volume jumps were determined as in figure 1.

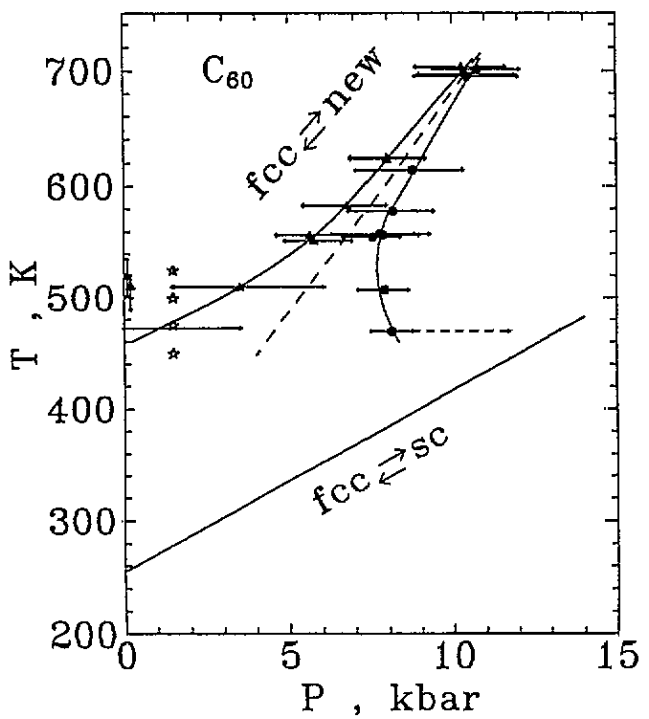

Figure 3. The T–P phase diagram of the C_{60} fullerite. Transitions on compression are marked with circles, and triangles are for reverse transitions. The horizontal dashed bar at 470 K shows the interval where a sluggish transition process was assumed from drifting gauge readings. Points over 578 K are least-squares fitted with straight lines. The midline is dashed. Stars mark the region where friction could be estimated only approximately rather than from the experimental isotherms. Heating points are away from the temperature axis for the same reason. The experimental line of the FCC-to-SC transition [8] is also drawn.

the equilibrium transition line. The latter is usually defined as the midline of the hysteresis region. The equilibrium line thus obtained has a slope dT/dP = 38.7 K kbar^{-1}. Its linear extension intersects the temperature axis near room temperature.

The equilibrium line of the orientational transition to 14 kbar is plotted in figure 3 after Samara *et al* [8]. They observed a break in the line slope (to 2.8 K kbar^{-1}) at this pressure, then the heat peak they fixed was gradually suppressed in three heating/cooling cycles. It seems evident from the T–P diagram that these phenomena over 14 kbar could be due to accumulation of the new phase found here rather than the reaction with the pressure-transmitting medium they assumed.

3.2. The compressibility of two C_{60} phases at 290 K

The compressibility of C_{60} phases involved could be conveniently compared in the same experiment. For this purpose, the new phase was quenched from 560 K at P = 20 kbar. Then the sample was decompressed and cycled to 27 kbar at 290 K. The FCC phase was recovered by heating to 610 K at P = 1 bar. Compressibility cycles were the same. The gauge readings at the same applied pressure were averaged between compression and decompression in each cycle, then volume changes were calculated. The compressibility of the pressure cell and the Al cover was measured in a special experiment and taken into account. The initial specific volume of the new phase was accepted to be 0.85 V_0.

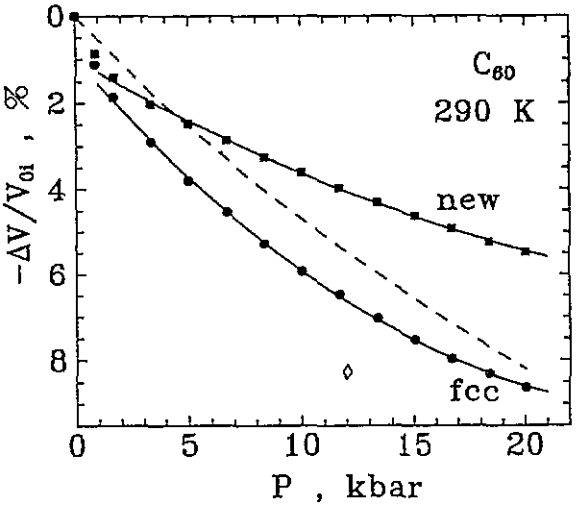

Figure 4. The pressure–volume relationships for the new C_{60} phase and for the recovered FCC phase at 290 K. Least-squares fits with the second-order polynomials are plotted in solid lines. The dashed curve shows the x-ray equation of state to 200 kbar [10]. The other point (diamond) is from [19].

Figure 4 represents the baric dependence of volumes for the new and recovered FCC phases. Approximation with second-order polynomials is fairly good, except for pressures $P \leqslant 2$ kbar where both phases showed enormous compressibility. It is clear from figure 4 that the different compressibility of C_{60} phases gives the main contribution to the unusual difference in volume jumps at high and atmospheric pressures. Isothermal bulk moduli were estimated from the polynomial coefficients: K_T = 329 kbar for the new phase and K_T = 164 kbar for the recovered FCC one. The latter value agrees with that obtained from the x-ray data up to 200 kbar (K_T = 181 kbar [10]). Correlation of the present $V(P)$ curve

with the equation of state of Duclos *et al* [10] is fairly good, except for $P \leqslant 2$ kbar again. We assume that the high initial compressibility is correlated with the lack of a volume jump due to the orientational transition anticipated at about 2 kbar. The rather normal behaviour of $V(P)$ in this range at elevated temperatures (figure 1) partly confirms this assumption.

3.3. The x-ray diffraction spectra

The FCC lattice parameter of as-prepared C_{60}, $a_0 = 14.17$ Å, coincided with the earlier data [5]. Figure 5 shows x-ray diffraction patterns taken at 295 K from the same C_{60} sample, but in different phase states. The *as-quenched* sample (top) was retained in the new phase after compressibility measurements by means of cooling from 700 to 290 K under $P = 20$ kbar and decompression. To avoid deformation of the sample, we removed the Al cover on one side only. The Al cover walls round the sample contributed to the spectrum. A similar spectrum was obtained from another sample quenched under hydrostatic pressure in a teflon ampoule (one extra reflection from teflon superposed the C_{60} spectrum).

Al reflections were eliminated when the sample was crushed out from the cover and *ground* (middle). The bottom spectrum gives evidence that the FCC phase was recovered after vacuum annealing the ground sample at 620 K, but its lattice parameter was $a_0 = 14.12$Å. It is obvious from comparison of the strong peaks in the three spectra that the sample ground at 295 K was two phase. This is indicative of a partial transition due to grinding at room temperature as well as of a single-phase state of the as-quenched sample, crystalline phases taken into account. Identification of the crystal structure of the new phase is in progress.

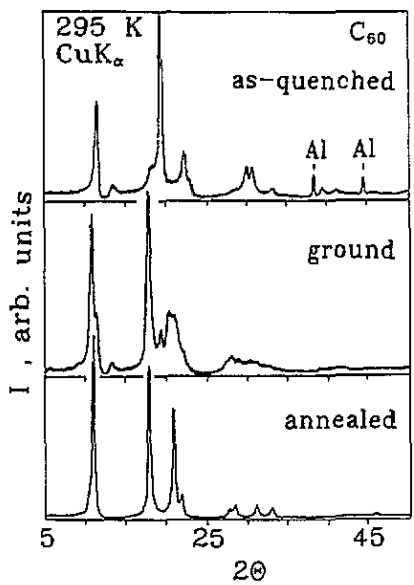

Figure 5. X-ray diffraction patterns from the same C_{60} sample in three phase states. Top: the *as-quenched* new phase. Al peaks are from the cover walls round the sample. Middle: a two-phase state in the *ground* sample. Bottom: the recovered FCC phase in the *annealed* sample.

3.4. Heat capacity

Figure 6 represents prominent features in the heat capacity curves, $c_p(T)$, for three phase states of C_{60}. There was rather good correlation between the low-temperature and high-temperature runs in the interval where they overlapped, 350–420 K, but the agreement was

not complete. The $c_p(T)$ curves were computer averaged and smoothed in this interval (shown in dashed lines).

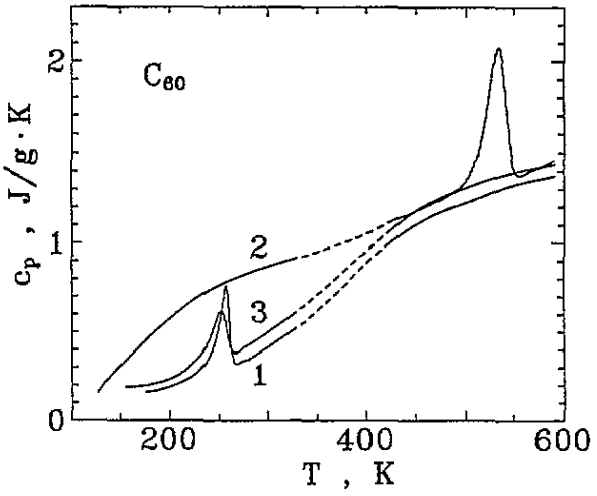

Figure 6. The heat capacity $c_p(T)$ of solid C_{60}: 1, the as-prepared powder; 2, the new phase; 3, the recovered FCC phase.

The heat capacity $c_p(T)$ of the as-prepared C_{60} showed the well known sharp peak due to the orientational transition with a maximum at $T_c = 257$ K (curve 1). Precursory anomalous behaviour of $c_p(T)$ was evident over 220 K. The total heat effect between 220 and 268 K was $\Delta H = 9.6$ J g^{-1}. This is in accord with other data [5–7].

The new phase had much larger heat capacity below room temperature, but the $c_p(T)$ dependence was smooth (curve 2). The latter is not surprising because lowered librational freedom is implicit from higher density. A large endothermal peak occurred between 500 and 550 K with a maximum at $T \simeq 530$ K. A precursory anomaly of $c_p(T)$ could also be assumed; it was unambiguous over 470 K. Taking into account the difference in heating rates, there is a close correspondence of the observed transition interval to that in volume measurements. The total heat effect at 470–550 K ranged in five experiments between 19.6 and 26.8 J g^{-1}. We assume that this rather large scatter is due to the nature of the new phase, hence, due to parameters of its preparation.

The $c_p(T)$ dependence of the recovered FCC phase (curve 3) was very similar to that of the as-prepared C_{60}, but the heat peak of the orientational transition became less sharp. Its maximum shifted to 244.4 K, and the precursory anomaly began at 190 K. The heat effect between 190 and 270 K was reduced to $\Delta H = 4.9 \pm 0.2$ J g^{-1}. It can be concluded from the modified parameters of the orientational transition as well as from the modified lattice parameter that recovery to the FCC phase after annealing at 620 K is imperfect.

4. Discussion

Two exciting questions arose from the experimental data. The first one is: what phase is thermodynamically stable somewhat below room temperature? The Clausius–Clapeyron equation cannot give any hint because the transition from the new phase to the FCC one occurs far from the equilibrium point at atmospheric pressure. Partial transition due to grinding was indicative of metastability of the new phase at 295 K. Therefore, we cooled another sample of the new phase and a mortar to about 220 K and ground the sample at this

temperature. Partial transition of this sample was evident again from the x-ray diffraction spectrum. It seems therefore that the equilibrium line in figure 3 cannot be linearly extended to zero pressure, but deflects to low temperatures at $P < 5$ kbar. A special study is necessary to determine the range of thermodynamic stability of the new phase.

The other question is connected with a large volume jump: the new phase is more dense than the recovered FCC one by 8.5%, and the latter is more dense than the initial phase by ~1%. What rearrangement of a close-packed FCC lattice could cause this increase in density? Origination of chemical binding between the C_{60} molecules in the new phase was a likely explanation for the large volume jump as well as for imperfect recovery to the FCC phase and kinetic phenomena associated with the new transition. To test this assumption, we attempted to dissolve several of our samples in toluene. The new phase was ground to a fine powder at room temperature or at 77 K. These powders were absolutely insoluble in toluene at ambient conditions over a period of a week. The same powder was heated to 600 K to recover the FCC phase. Then it readily dissolved in toluene: 80% in 12 h at room temperature and total dissolution in boiling toluene. The deep-violet solution obtained had the ultraviolet–visible spectrum characteristic of pure C_{60}. This result argues in favour of C_{60} polymerization in the new phase.

Acknowledgments

The research described in this publication was made possible in part by grants from the International Science Foundation No REN 000 and No REP 000.

References

[1] Dworkin A, Szwarc H, Leach S, Hare J P, Dennis T J S, Kroto H W, Taylor R and Walton D R M 1991 *C. R. Acad. Sci., Paris* II **312** 979–82
[2] Heiney P A, Fischer J E, McGhie A R, Romanow W J, Denenstein A M, McCauley J P Jr, Smith A B III and Cox D E 1991 *Phys. Rev. Lett.* **66** 2911–4
[3] Sachidanandam R and Harris A B 1991 *Phys. Rev. Lett.* **67** 1467
[4] David W I F, Ibberson R M, Dennis T J S, Hare J P and Prassides K 1992 *Europhys. Lett.* **18** 219–25
[5] Heiney P A, Vaughan G B M, Fischer J E, Coustel N, Cox D E, Copley J R D, Neumann D A, Kamitakahara W A, Creegan K M, Cox D M, McCauley J P Jr and Smith A B III 1992 *Phys. Rev.* B **45** 4544–7
[6] Atake T, Tanaka T, Kawaji H, Kikuchi K, Saito K, Suzuki S, Ikemoto I and Achiba Y 1991 *Physica* C **185–189** 427–8
[7] Kriza G, Ameline J-C, Jérome D, Dworkin A, Szwarc H, Fabre C, Schütz D, Rassat A, Bernier P and Zahab A 1991 *J. Physique* I **1** 1361–4
[8] Samara G A, Hansen L V, Assink R A, Morosin B, Schirber J E and Loy D 1993 *Phys. Rev.* B **47** 4756–63
[9] Samara G A, Schirber J E, Morosin B, Hansen L V, Loy D and Sylwester A P 1991 *Phys. Rev. Lett.* **67** 3136–9
[10] Duclos S J, Brister K, Haddon R C, Kortan A R and Thiel F A 1991 *Nature* **351** 380–2
[11] Yamawaki H, Yoshida M, Kakudate Y, Usuba S, Yokoi H, Fujiwara S, Aoki K, Ruoff R, Malhotra R and Lorents D 1993 *J. Phys. Chem.* **97** 11 161–2
[12] Yoo C S and Nellis W J 1992 *Chem. Phys. Lett.* **198** 379–82
[13] Núñez-Regueiro M, Monceau P and Hodeau J-L 1992 *Nature* **355** 237–9
[14] Núñez-Regueirio M, Abello L, Lucazeau G and Hodeau J-L 1992 *Phys. Rev.* B **46** 9903–5
[15] Yoo C S and Nellis W J 1991 *Science* **254** 1489–91
[16] Snoke D W, Raptis Y S and Syassen K 1992 *Phys. Rev.* B **45** 14 419–22
[17] Bashkin I O, Rashchupkin V I, Kobelev N P, Moravsky A P, Soifer Ya M and Ponyatovsky E G 1994 *JETP Lett.* **59** 258–61 (in Russian)
[18] Aptekar I L, Rashchupkin V I, Tonkov E Yu and Ponyatovsky E G 1977 *Sov. Phys.–Solid State* **19** 3180–4
[19] Fischer J E, Heiney P A, McGhie A R, Romanow W J, Denenstein A M, McCauley J P Jr and Smith A B III 1991 *Science* **252** 1288–90